

Structural Analysis of Ball-milled Graphite by Molecular Orbital Calculation

T. Kaneyoshi, M. Motoyama^a and T. Tanaka^b

^aHyogo Prefectural Institute of Industrial Research, 3 Yukihiro-cho, Suma-ku, Kobe 654 JAPAN

^bOsaka Sangyo University, 3 Nakagaito, Daito, Osaka 574, JAPAN

Ball-milling of graphite powder was carried out by using a stainless ball-mill. A microcrystalline structure was observed in the ball-milled graphite. C K x-ray emission spectra of ball-milled graphite were measured by an electron probe microanalyzer (EPMA). C K x-ray emission spectra were compared with C2p partial electron densities of states (DOS) calculated by the Discrete-Variational (DV) Hartree-Fock-Slater (X α) molecular orbital (MO) method. The results of MO calculation suggested that refinement of the graphite powder occurred up to 1000hr of milling while keeping graphite structure. 2000hr-milling changed the C-C bonding states of graphite.

1. INTRODUCTION

Mechanical alloying/milling (MA/MM) processes are the solid-state reaction techniques to procedure nonequilibrium phases such as amorphous[1-2], metastable compounds[3-4] and supersaturated solid solutions[5]. We already reported the formation processes of metastable carbides for some metal-carbon alloy systems[4-8]. In the case of the high carbon Fe-C system, we found amorphization of graphite. The structure change of graphite during the MA process, however, had not yet been revealed.

Carbon has been used widely as an industrial material, because of the diversity in chemical combination and structure. The typical atomic structures of carbon can be seen in three allotropic forms; amorphous carbon, graphite and diamond. In addition, such fullerene as C₆₀[9-10] was newly found as the fourth allotropic form of carbon in recent years. It is also reported that carbon forms various intermediate states of these structures, particularly between amorphous carbon and graphite. So, it is very interesting that how graphite change its structure by MA/MM processes.

In this paper, structure change of graphite powder in MM process will be reported. Structure change of carbon atom will also be discussed from the results of molecular orbital (MO) calculation.

2. EXPERIMENTAL

The graphite powders(99.9at%, grain size:5 μ m) were charged in a stainless steel ball-mill, and were mechanically ground (MG) in an argon atmosphere. The graphite powders which were ground after various times had been studied by transmission electron microscopy(TEM) and x-ray diffractometry.

Using an EPMA, C K x-ray emission spectra were measured on the ground graphite powders which were pressed onto aluminum plate at an acceleration voltage of 15kV and a sample current of 0.2mA. A multilayer pseudo-crystal of lead stearate (2d=10nm) was used as an analyzing element. The C K x-ray emission spectra were detected with a flow type proportional counter and recorded on a strip chart after passing through a pulse height analyzer in order to prevent from the overlap of the spectrum of other elements on the C K x-ray spectrum.

We apply the method of Manne[11] and Urch[12] and use DV-X α MO calculation method originally written by Adachi and co-workers [13-14] to calculate C K x-ray emission spectrum. C K x-ray emission spectrum reflects a density of states (DOS) of C2p, because this spectrum is generated by the transition of electrons from C2p to C1s and the dipole selection rule holds within an atom. Consequently, we describe the C K x-ray intensity as follows;

$$I \propto \sum |c_{2p_x,jk}|^2 + |c_{2p_y,jk}|^2 + |c_{2p_z,jk}|^2 \quad (1)$$

($c_{2p_x,jk}$, $c_{2p_y,jk}$, $c_{2p_z,jk}$: MO coefficient of the carbon $2p_x$, $2p_y$ and $2p_z$ orbitals)

Finally, we have broadened the calculated spectra by a convolution of Gaussian function. Figure 1 shows the graphite standard model used for the present calculation.

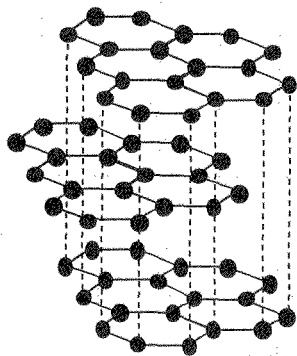


Fig.1 Graphite standard model for MO calculation

3. RESULTS AND DISCUSSION

Figure 2 shows lattice images of the graphite powders ground after various times. A fine grain was observed in the graphite powders ground after 100hr of milling. However, a graphite lattice was yet clearly observed. After 2000hr and 5000hr of milling, a graphite lattice was disordered.

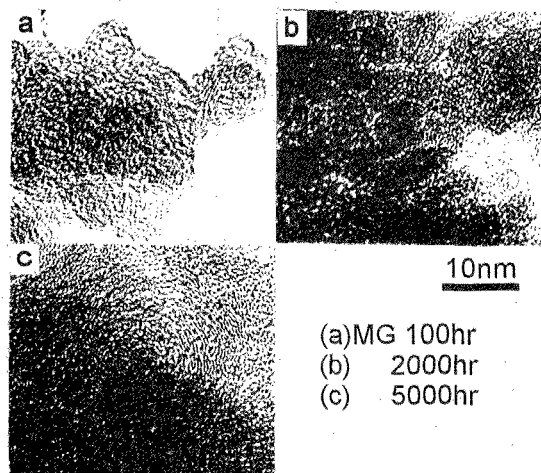


Fig.2 Lattice images of the graphite powders ground after various times.

Figure 3 shows x-ray diffraction patterns of the graphite powders ground after various times. The diffraction peaks of the graphite disappeared after

1000hr of milling, and only hollow pattern was observed. After 3000hr of milling, the hollow peak of 002 diffraction line of graphite was shifted to low angle side. The intensity of the diffraction pattern decrease remarkably after 5000hr of milling. According to the previous works[4-8], appearance of the diffraction peaks which were observed at about 45° after 3000 and 5000hr of milling was considered to be due to the iron impurities ($\alpha\text{Fe } 110 \approx 44.6^\circ$) which were contaminated from the stainless steel ball-mill.

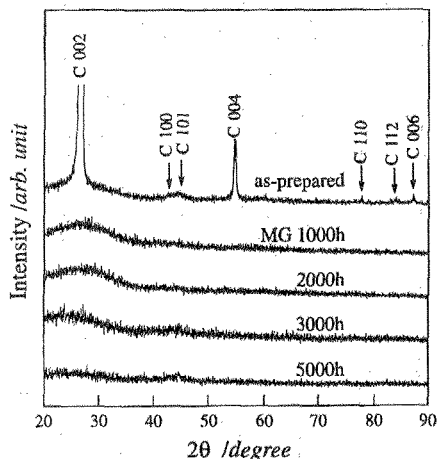


Fig. 3 X-ray diffraction patterns of the graphite powders ground after various times.

Figure 4 shows C K x-ray emission spectra obtained from the graphite powders ground after various times. The main-band is shifted to the high-energy side. The intensity of the high-energy sub-band (the shoulder at about 281eV) increased, and with increasing milling time from 100 to 1000hr of milling. After 2000hr of milling, the main peak position was shifted to the high-energy side moreover and overlapped with high-energy sub-band. After 3000 and 5000hr of milling, the main- and sub-bands separated and the shapes of the spectra were similar to those obtained from the graphite powders ground from 100 to 1000hr of milling.

The change of the spectra obtained from the graphite powders ground up to 1000hr of milling was understood by using the polarized emission mechanism, as follows.

The characteristic x-rays are emitted perpendicular to the orbital direction. The x-ray intensity against a take-off angle (angle of electron beam direction against the c-axis) is written as

$$I(E, \theta) = I\sigma(E) \left(\frac{1 + \cos^2 \theta}{2} \right) + I\pi(E) \sin^2 \theta \quad (2)$$

where θ is a take-off angle, and $I\sigma(E)$, $I\pi(E)$ are the x-ray intensities of σ and π orbitals, respectively. So, $I(E, \theta)$ changes with the value of the take-off angle, θ .

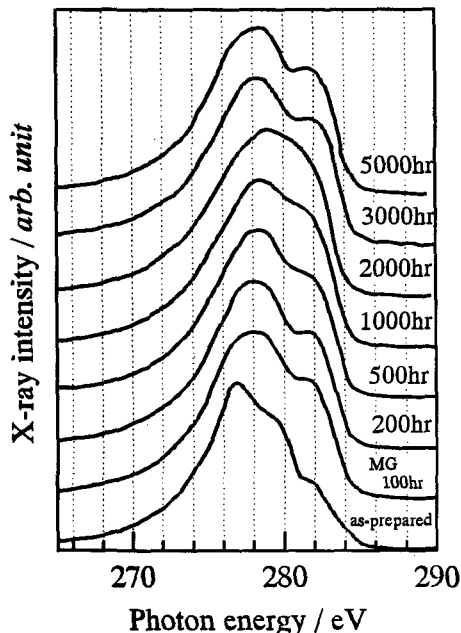


Fig. 4 C K x-ray emission spectra obtained from the graphite powders ground after various times.

Figure 5 shows the schema of the polarized emission effect on the C K x-ray emission spectra in case of the graphite powders. Since the particles of as-prepared graphite powders are relatively large, the c-axis is oriented horizontally to electron beam direction by pressing onto aluminum plate. This geometry corresponds to a smaller θ value and so the information of σ orbital was obtained. When the particles of the graphite powders become small and equiaxed by milling, the c-axis is oriented randomly although the powders are pressed and average θ value tends to become larger.

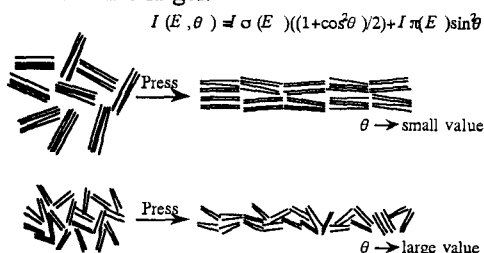


Figure 5 Schema of the polarized emission effect on the C K x-ray emission spectra.

Figure 6 shows C2p DOSs which are calculated for the graphite standard model of Fig.1 and combined σ and π components according to equation (2). When comparing the calculated spectra with the measured spectra, the result of calculation at $\theta=0^\circ$ and 45° explained the spectra obtained from the as-prepared graphite powders and the graphite powders ground from 100 to 1000hr of milling, respectively. It means that the application of the polarized emission mechanism is correct and refinement of the graphite powder occurred for up to 1000hr of milling while keeping the graphite structure.

However, the spectrum obtained from the graphite powders ground after 2000hr of milling was not able to be understood by using the polarized emission

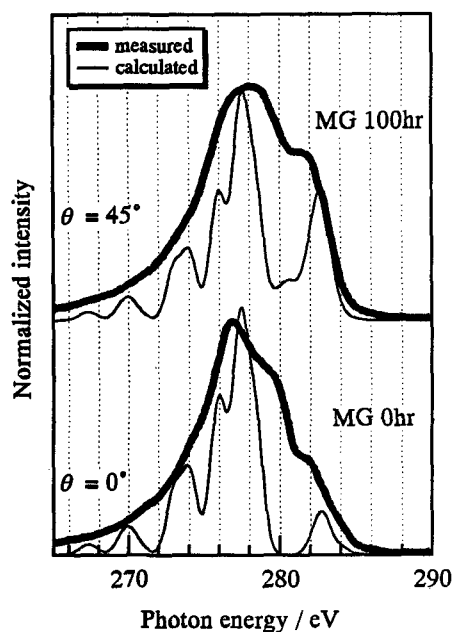


Fig. 6 C2p DOSs which are calculated for Fig.1 and combined σ and π components according to eq. (2).

mechanism. The various C2p DOSs were calculated for the models taken account of shear, press and disorder phenomena which might occur by milling. The arrangement and spacing of graphite layer were changed while keeping the planner carbon bonding in the shear and press models, respectively. On the other hand, we used the disorder model in which zigzag c-c chain predominated. The disorder model explained the spectrum obtained from the graphite powders ground after 2000hr of milling among those models. Figure 7

shows disorder model for carbon cluster and its $C2p$ DOS compared with the one for the standard model. Figure 8 shows σ and π components of $C2p$ DOS calculated for the disorder model against those for the standard model. The change of σ component contribute to high-energy side shift of the main peak position. The calculation models used in this work do not consider all phenomena which might occur by

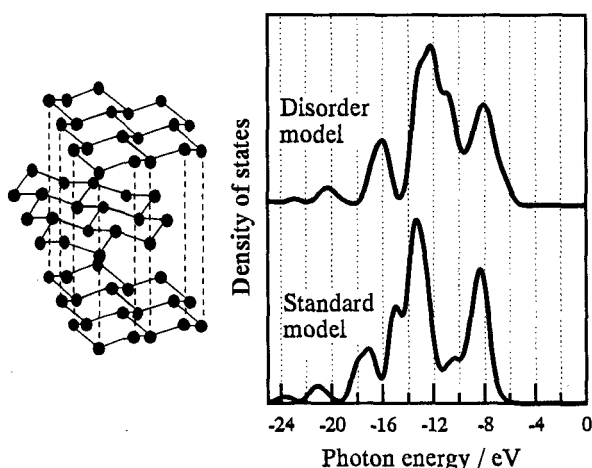


Fig.7 Disorder model for carbon cluster and its $C2p$ DOS compared with the one for the standard model.

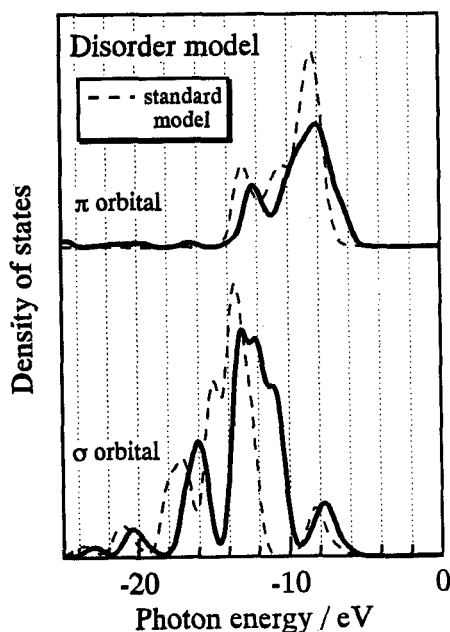


Fig. 8 σ and π components of $C2p$ DOS calculated for the disorder model compared with those for the standard model.

milling. But we could not at least explain the change of the spectrum, if the bonding states within graphite layer were not considered to be changed. So, it was suggested that 2000hr-milling changed the C-C bonding states of graphite.

4. CONCLUSIONS

Structure change of graphite powder in MM process were discussed from the results of measurement of x-ray emission spectra and MO calculation. The change of the spectra obtained from the graphite ground from 100 to 1000hr of milling was understood by using the polarized emission mechanism. It was considered that refinement of the graphite powder occurred up to 1000hr of milling while keeping graphite structure. The spectrum obtained from the graphite powders ground after 2000hr of milling was understood by using MO calculation model which was taken account of disorder phenomenon. It was suggested that 2000hr-milling changed the C-C bonding states of graphite.

5. REFERENCES

1. A. W. Weeber and H. Bakker; Phys. B, 153 (1988), 93.
2. *Mechanical Alloying*, ed. by P. H. Shingu; Mater. Sci. Forum, 88-90 (1992).
3. H. Okumura, K. N. Ishihara, P. H. Shingu, H. S. Park and S. Nasu; J. Mater. Sci., 27 (1992), 153.
4. T. Tanaka, S. Nasu, K. N. Ishihara and P. H. Shingu; J. Less Common Metals, 171 (1991), 237.
5. T. Tanaka, K. N. Ishihara and P. H. Shingu; Metall. Trans. A, 23A (1992), 2431.
6. T. Tanaka, S. Nasu, S. Imaoka, K. N. Ishihara and P. H. Shingu; J. Jpn. Soc. Powder Metall., 37 (1990), 660.
7. T. Tanaka, M. Motoyama, K. N. Ishihara and P. H. Shingu; Mater. Trans. JIM; 36 (1995) 276.
8. T. Tanaka, S. Nasu, K. Nakagawa, K. N. Ishihara and P. H. Shingu; Mater. Sci. Forum, 88 (1992), 269.
9. H. W. Kroto, J. R. Heath, S. C. O'Brien, R. F. Curl and R. Smalley; Nature, 318 (1985), 162.
10. W. Krätschmer, L. D. Lamd, K. Fostiropoulos and D. R. Huffman; Nature, 347 (1990), 354.
11. R. Manne, J. Chem. Phys., 52, 5733 (1970).
12. D. S. Urch, J. Phys. C, 3, 1275 (1970).
13. A. Rosén, D. E. Ellis, H. Adachi and F. W. Averill, J. Chem. Phys., 65, 3629 (1976).
14. C. Saito, M. Tsukada and H. Adachi, J. Phys. Soc. Jpn., 45, 1333 (1978).